Electronic Supplementary Material (ESI) for Journal of Materials Chemistry C.

Supporting Information: Rapid Predictions of the Colour Purity of Luminescent Organic Molecules

Shawana A. Ahmad [1], Julien Eng [1] and Thomas J. Penfold [1]

List of Figures

[1] Chemistry - School of Natural and Environmental Sciences, Newcastle University, Newcastle upon Tyne, NE1 7RU, UK, tom.penfold@ncl.ac.uk

List of Tables

S1 Supplementary Results: HOMO-LUMO Overlap

	$\mathcal{O}$	Λ	κ^2_{GS} / eV^2	κ^2_{S1} / eV^2	FWHM / eV	
					Theo.	Expt.
1	0.712	0.720	0.023	0.020	0.16	0.14 [1]
2	0.709	0.727	0.027	0.024	0.24	–
3	0.653	0.663	0.024	0.022	0.18	–
4	0.746	0.706	0.030	0.028	0.16	–
5	0.657	0.680	0.028	0.026	0.17	–
6	0.646	0.674	0.026	0.024	0.20	–
7	0.654	0.667	0.027	0.027	0.18	–
8	0.656	0.646	0.029	0.028	0.23	–
9	0.637	0.631	0.030	0.030	0.22	–
10	0.701	0.690	0.019	0.017	0.19	–
11	0.648	0.621	0.015	0.013	0.14	–
12	0.703	0.661	0.011	0.011	0.17	–
13	0.605	0.598	0.022	0.046	0.16	0.19 [2]
14	0.611	0.611	0.022	0.030	0.17	0.18 [3]
15	0.586	0.586	0.021	0.041	0.21	0.20 [3]
16	0.642	0.634	0.006	0.006	0.16	–
17	0.622	0.613	0.019	0.049	0.22	–
18	0.541	0.552	0.020	0.038	0.30	–
19	0.293	0.293	0.079	0.088	–	0.38 [4]
20	0.492	0.492	0.051	0.121	–	0.30 [4]
21	0.217	0.217	0.089	0.092	–	0.42 [4]
22	0.219	0.219	0.089	0.103	–	0.44 [4]
23	0.226	0.226	0.090	0.102	0.56	0.48 [4]
24	0.108	0.108	0.062	0.090	0.44	0.39 [5]
25	0.888	0.891	0.058	0.048	0.30	0.35 [6]
26	0.900	0.680	0.029	0.025	0.28	0.24 [7]
27	0.890	0.881	0.041	0.032	0.20	0.29 [8]

Table S1: $\mathcal{O}$ calculated at the ground state geometry. κ^2_{GS} κ^2_{S1} All other energies corresponds to emission, S_1 geometry.

S2 Supplementary Results: FWHM vs κ^2 Correlations

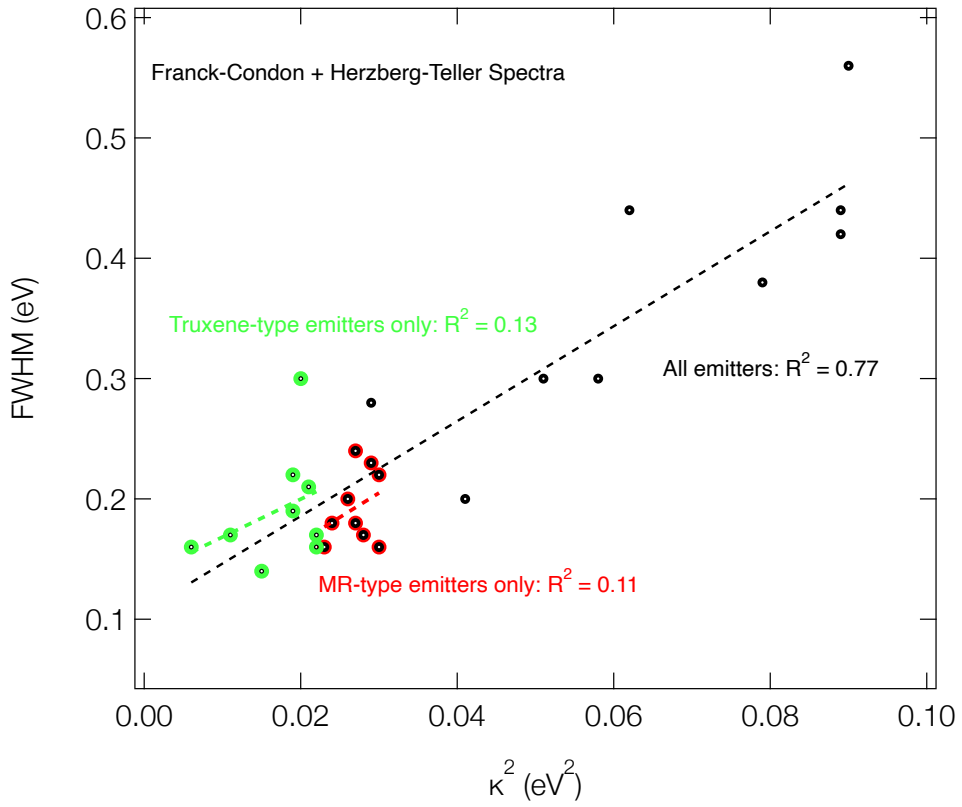

Figure S1: The correlation between emission FWHM and κ^2 analysed using the S_1 gradient at the ground state geometry. The dashed lined shows a linear fit to the data, excluding the data points based upon experimental FWHM. The black circles and dashed line corresponds to the data in Figure 6a. The green and red isolates the truxene and MR emitters, respectively.

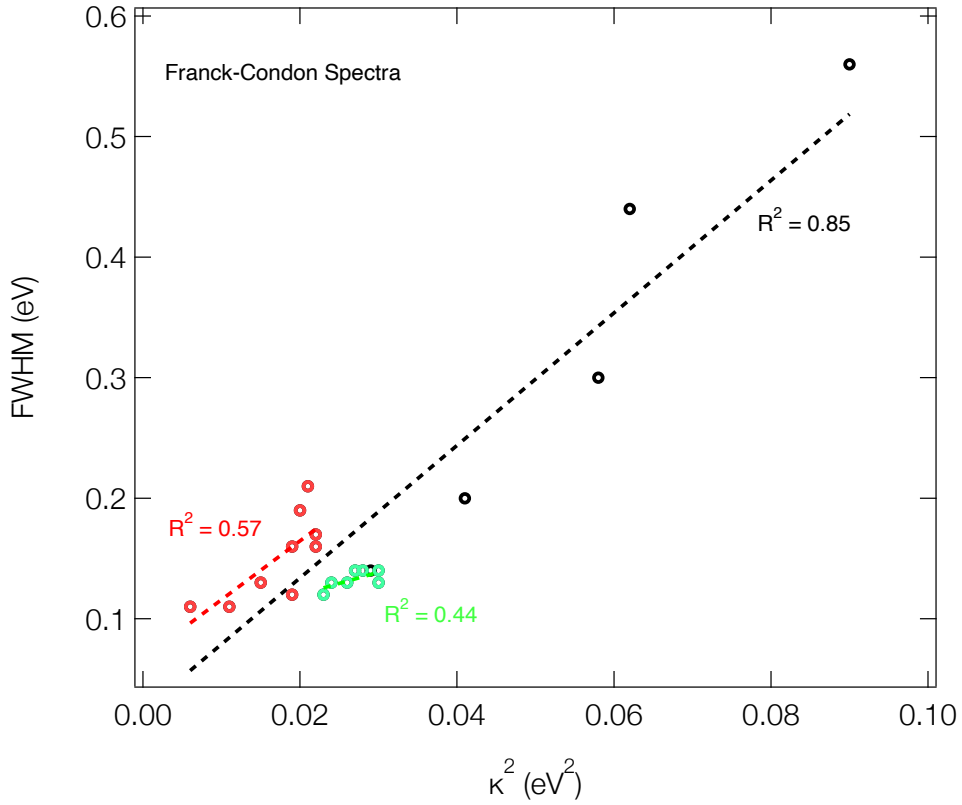

Figure S2: The correlation between emission FWHM of Franck-Condon only spectra and κ^2 analysed using the S_1 gradient at the ground state geometry. The dashed lined shows a linear fit to the data, excluding the data points based upon experimental FWHM. The black circles and dashed line corresponds to the data in Figure 6a. The green and red isolates the truxene and MR emitters, respectively.

S3 Supplementary Results: Emission Spectra

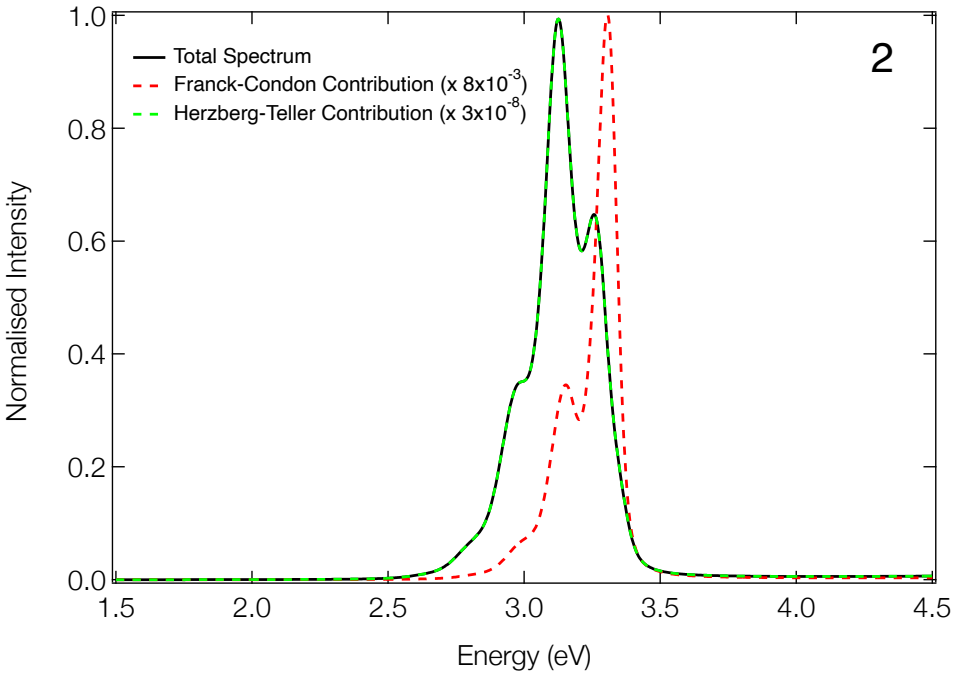

Figure S3: The computed emission spectrum of **2**.

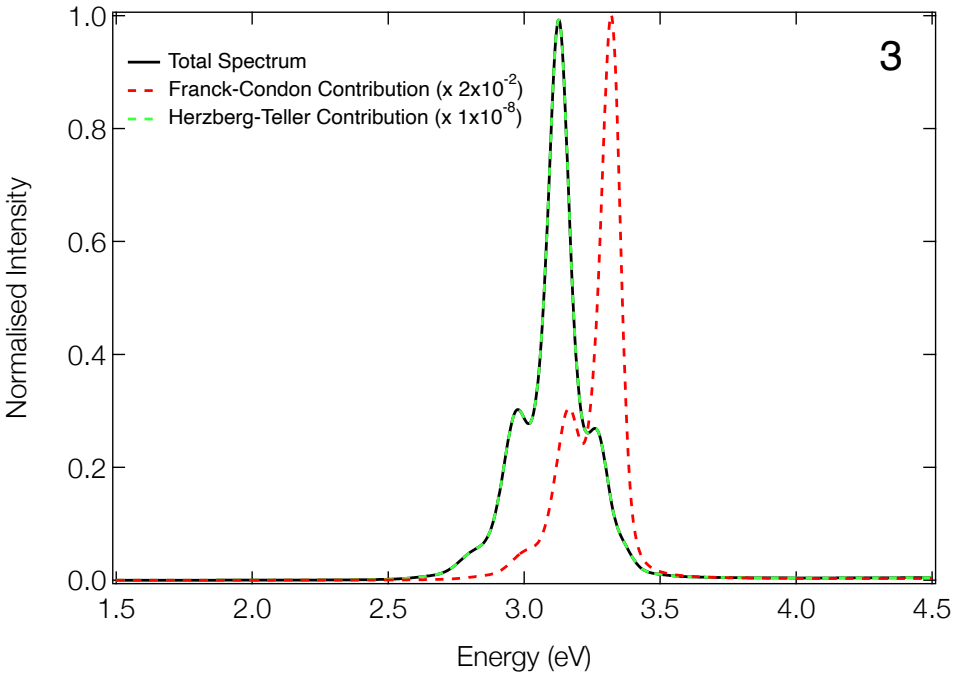

Figure S4: The computed emission spectrum of **3**.

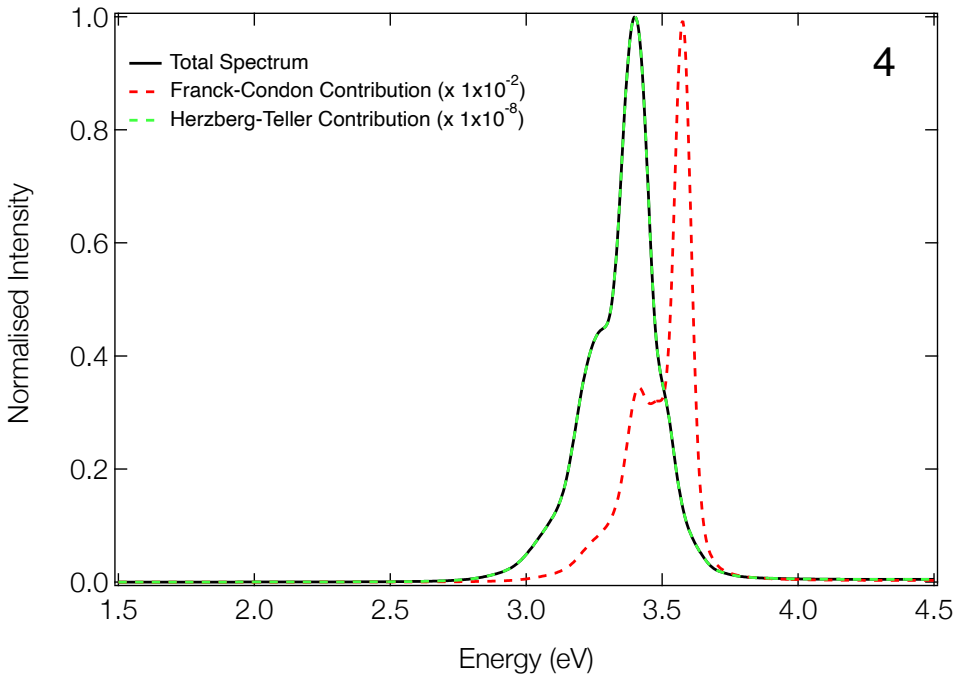

Figure S5: The computed emission spectrum of **4**.

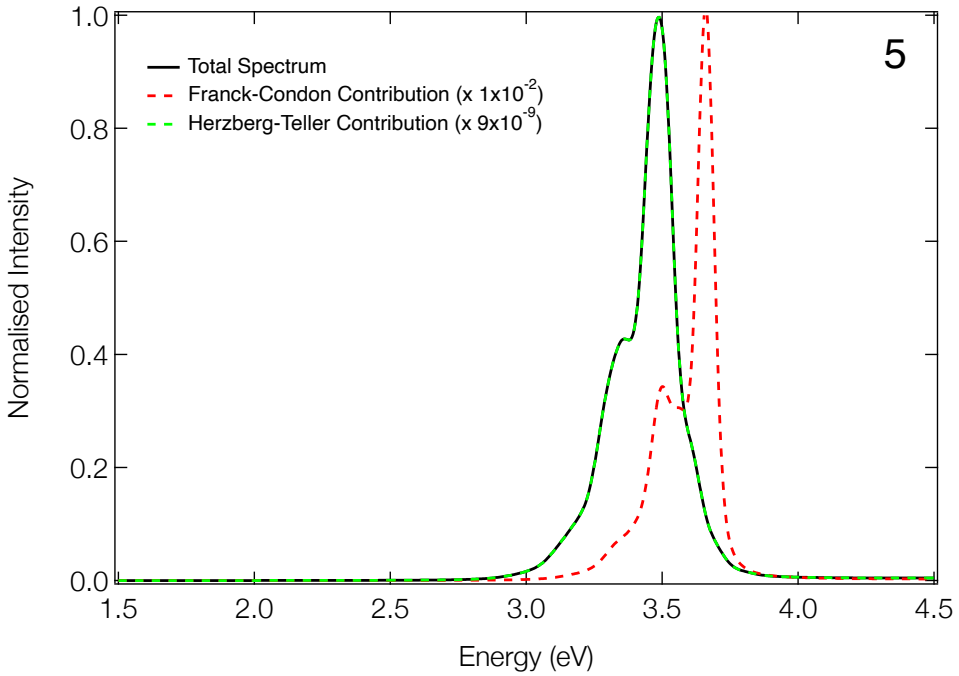

Figure S6: The computed emission spectrum of **5**.

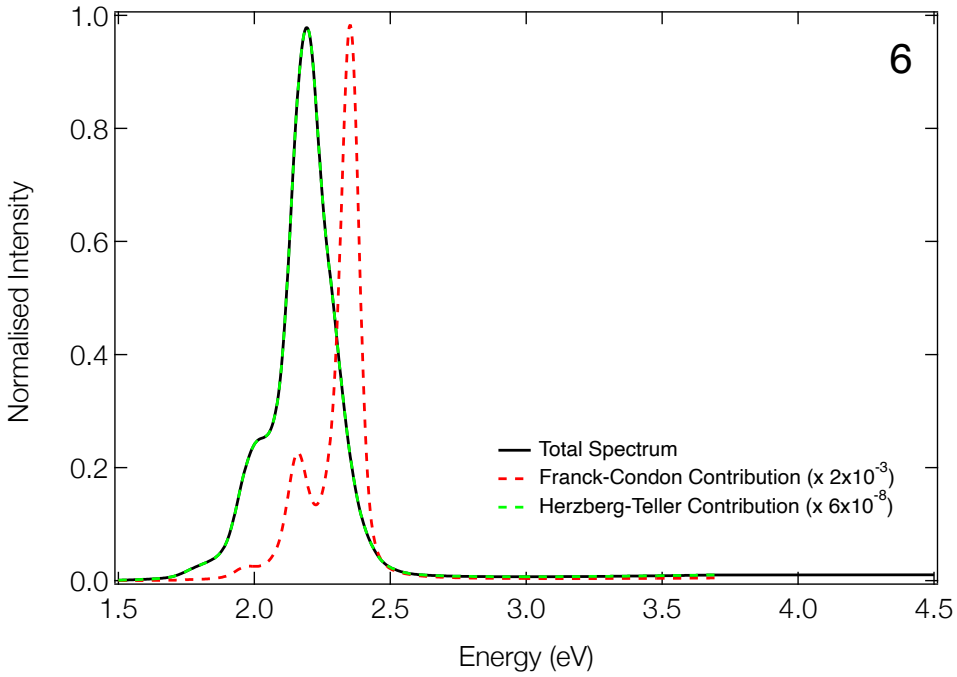

Figure S7: The computed emission spectrum of **6**.

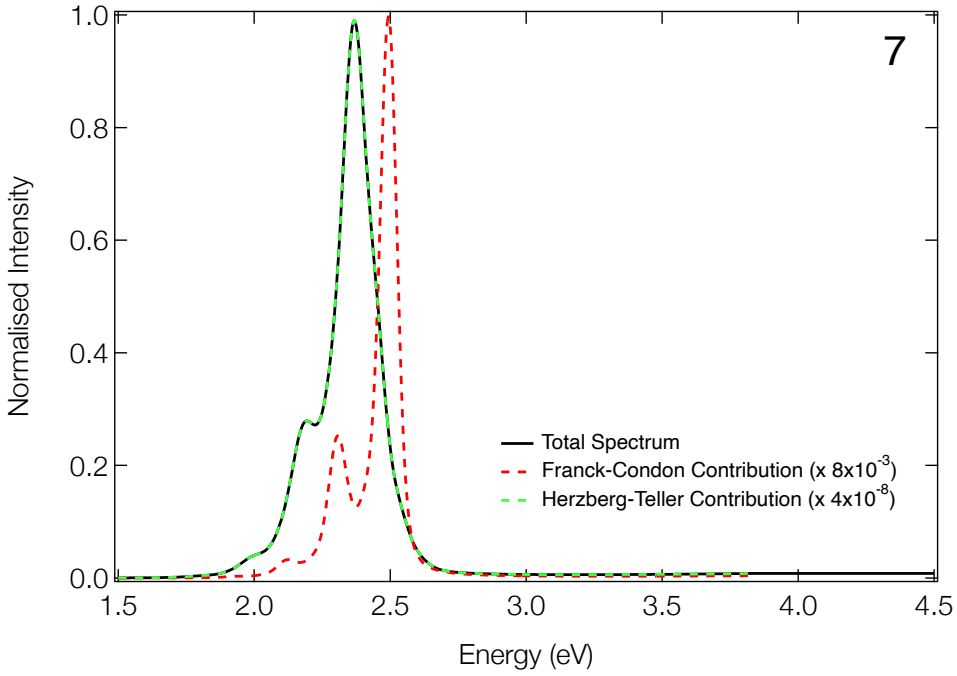

Figure S8: The computed emission spectrum of **7**.

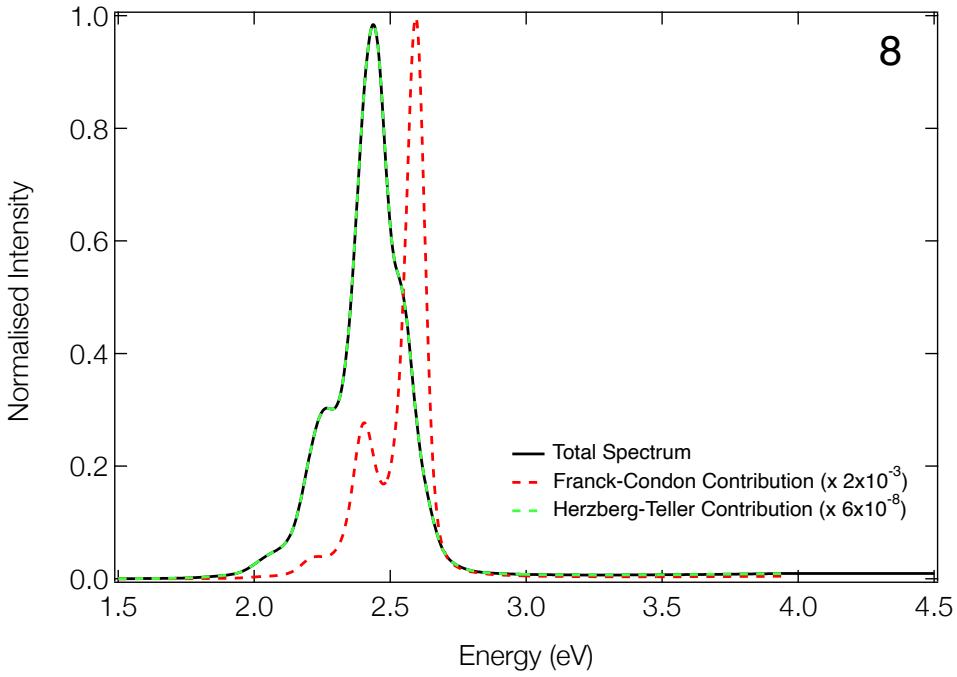

Figure S9: The computed emission spectrum of **8**.

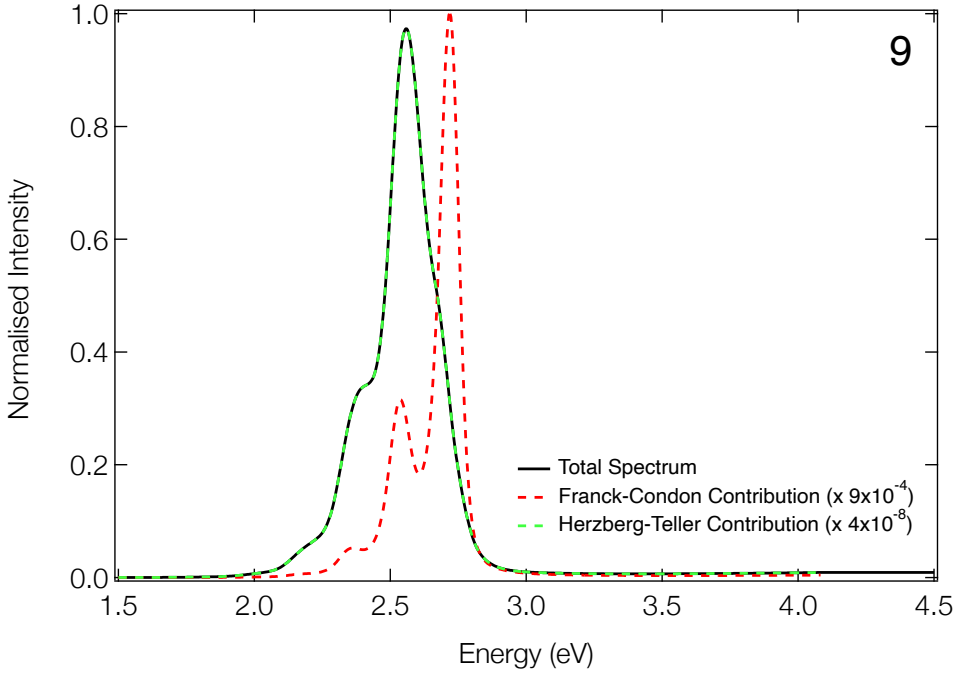

Figure S10: The computed emission spectrum of **9**.

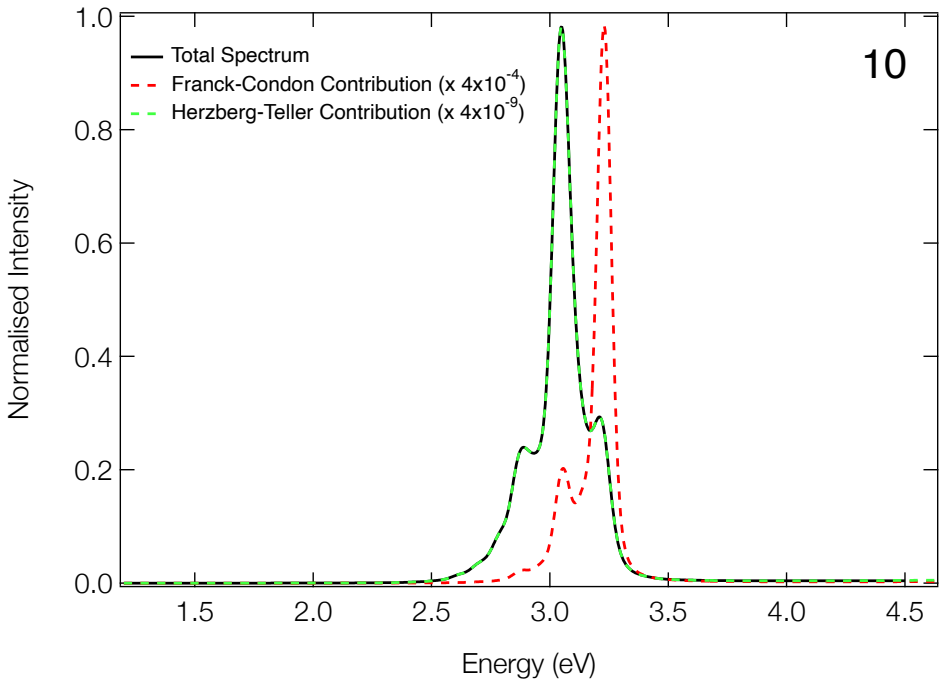

Figure S11: The computed emission spectrum of **10**.

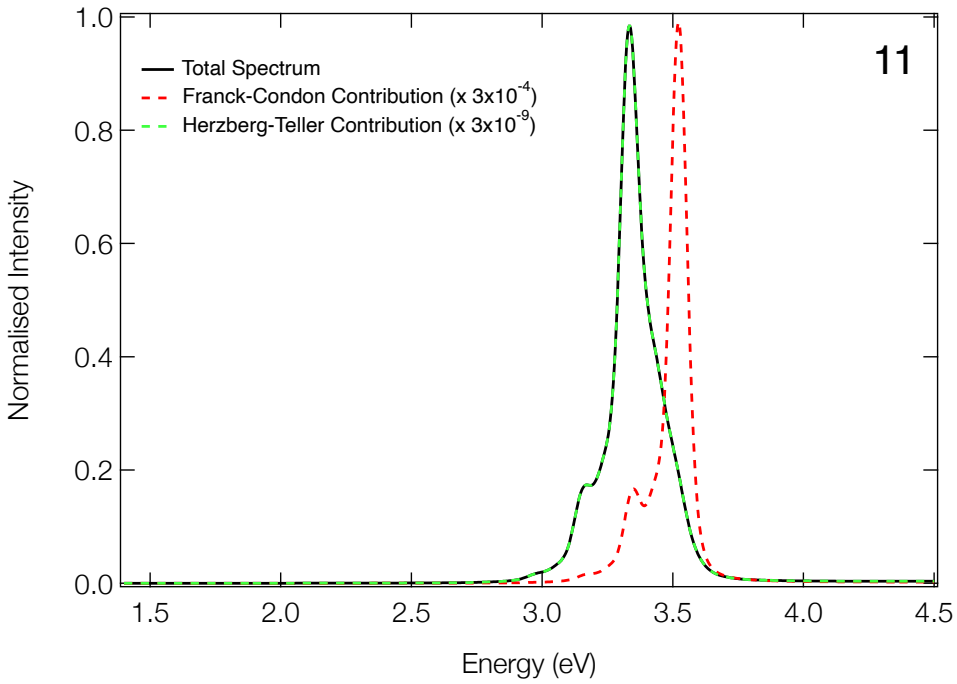

Figure S12: The computed emission spectrum of **11**.

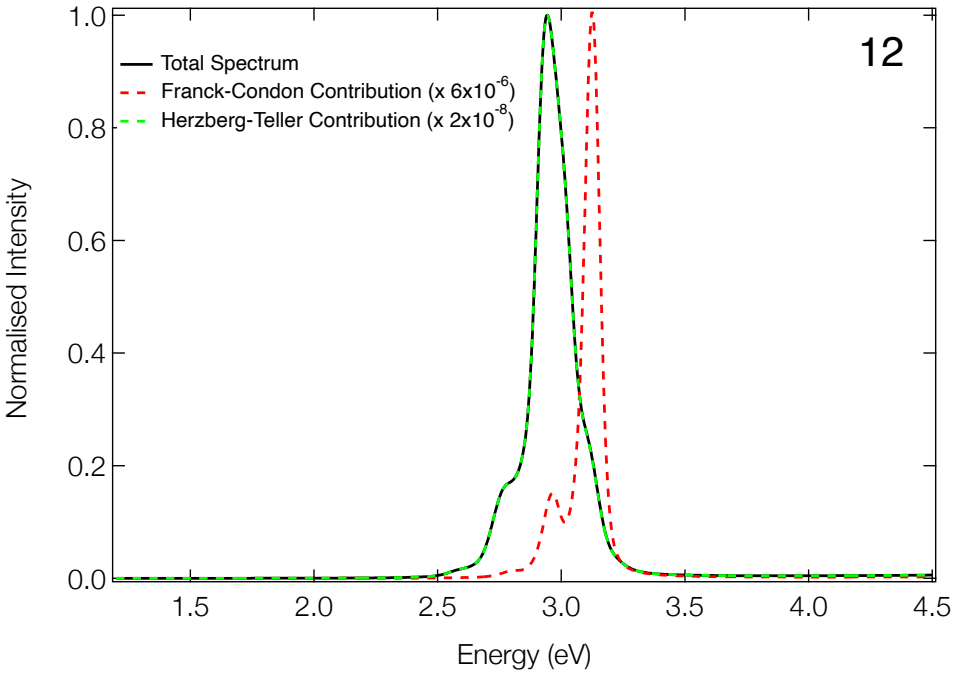

Figure S13: The computed emission spectrum of **12**.

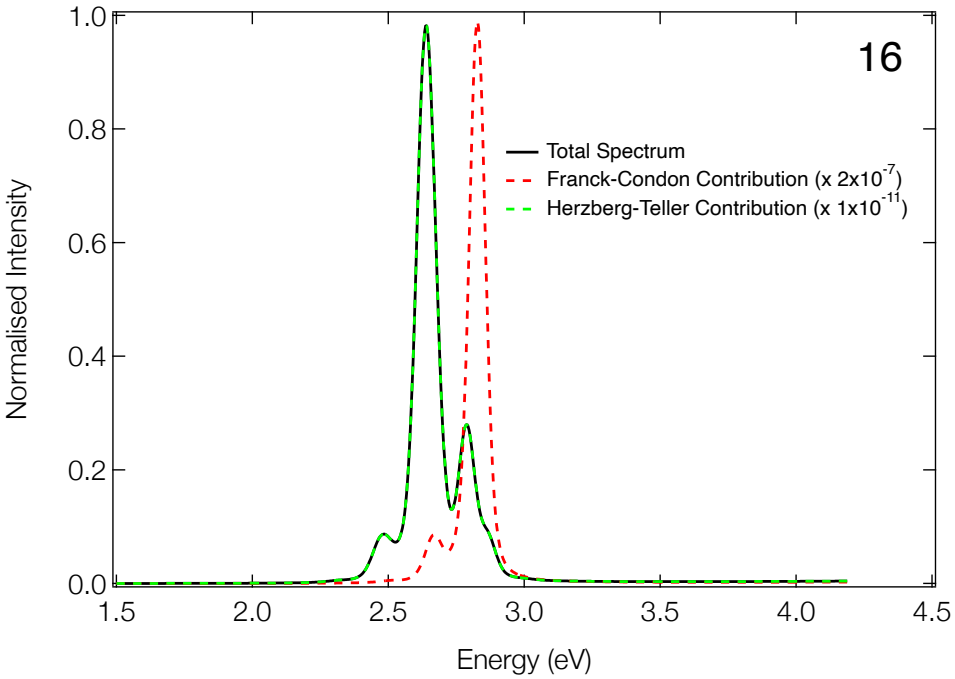

Figure S14: The computed emission spectrum of **16**.

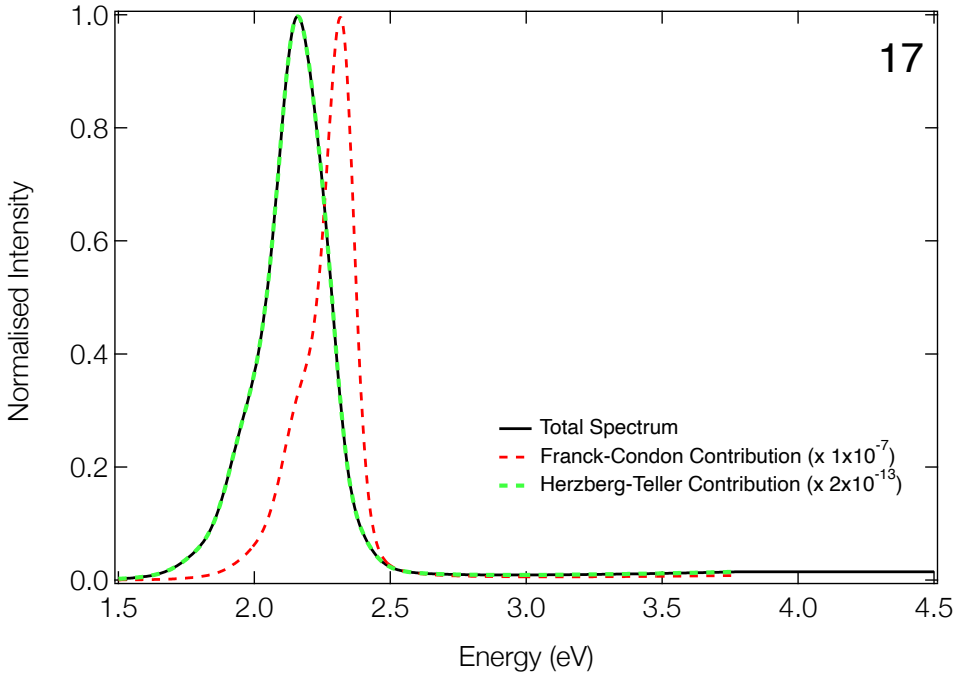

Figure S15: The computed emission spectrum of **17**.

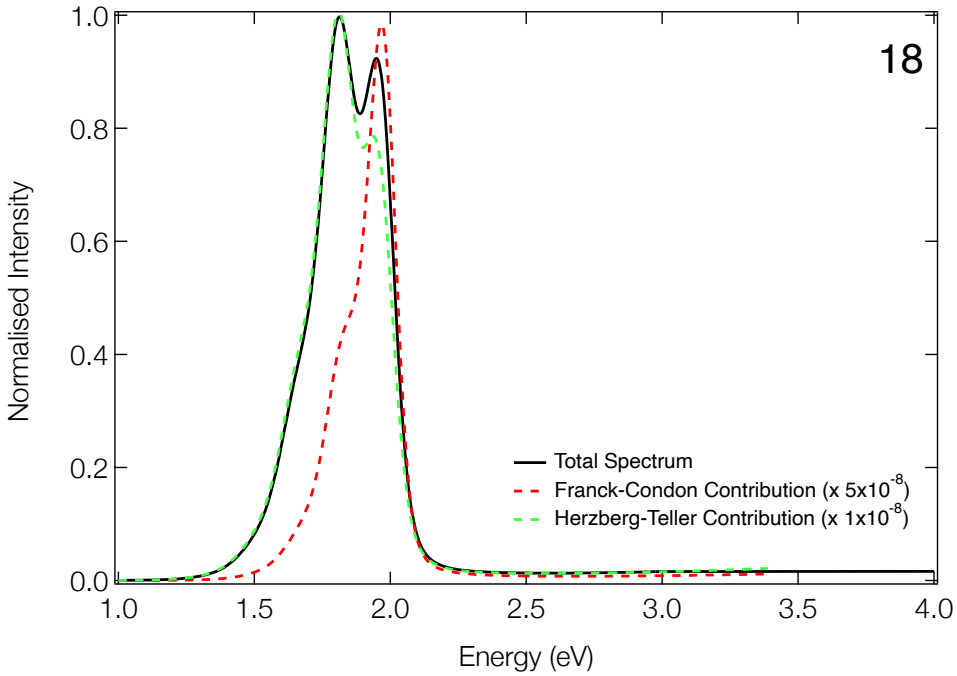

Figure S16: The computed emission spectrum of **18**.

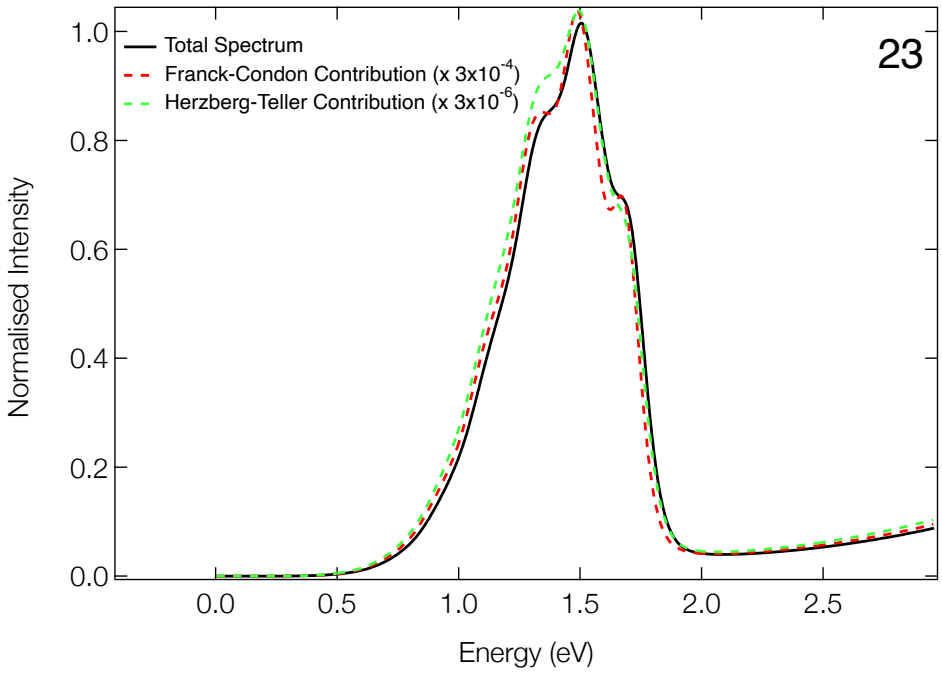

Figure S17: The computed emission spectrum of **23**.

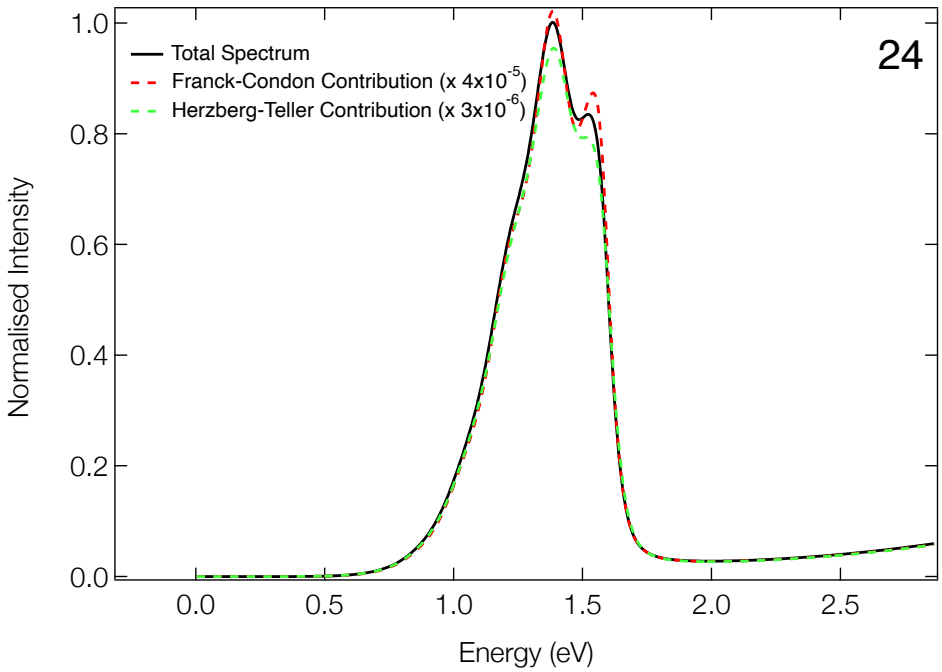

Figure S18: The computed emission spectrum of **24**.

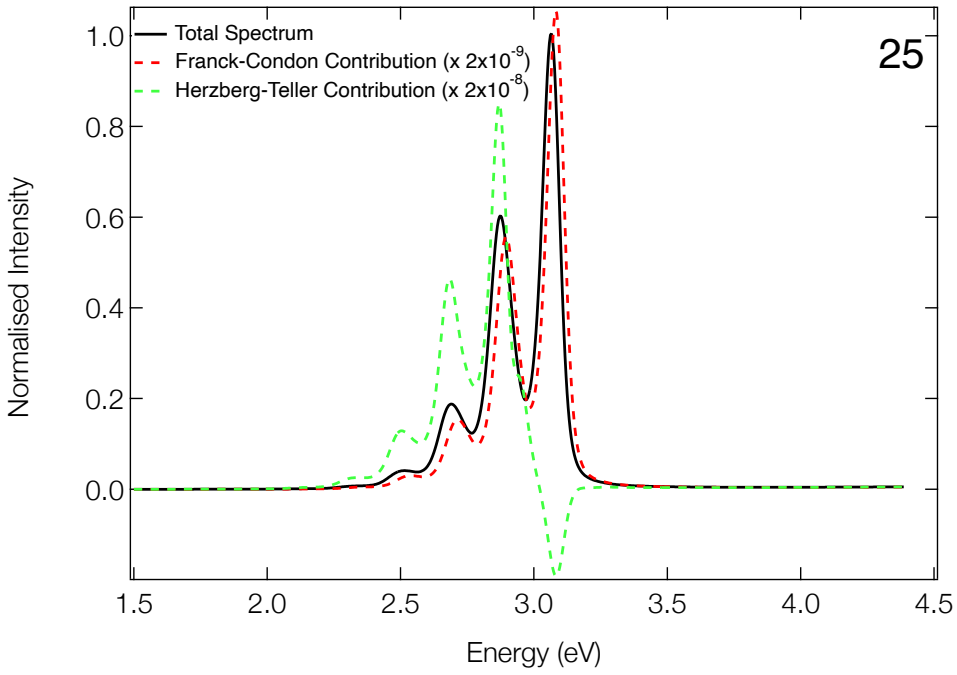

Figure S19: The computed emission spectrum of **25**.

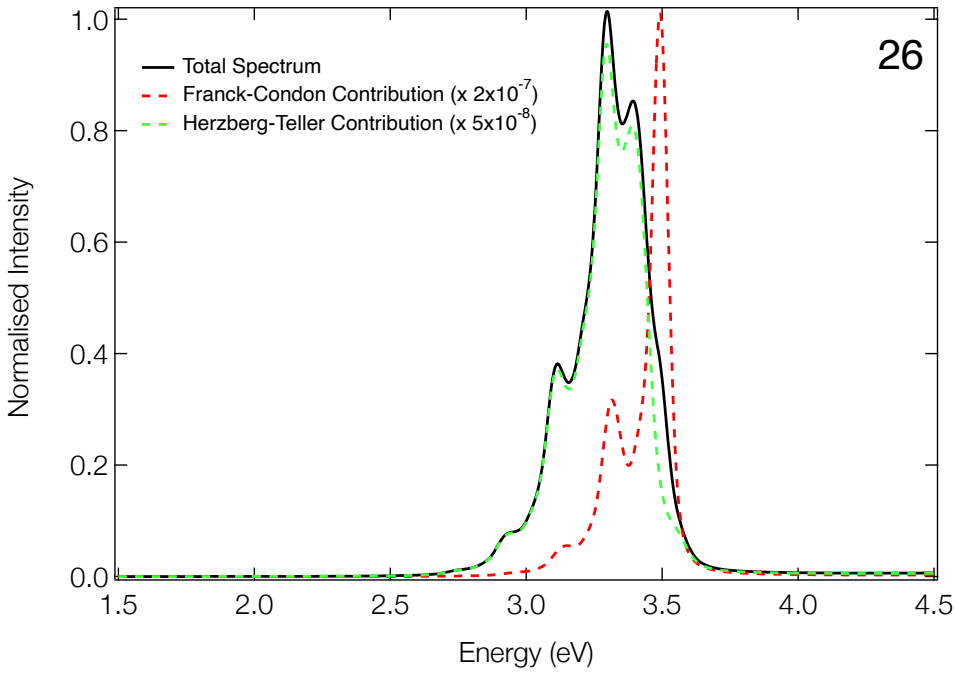

Figure S20: The computed emission spectrum of **26**.

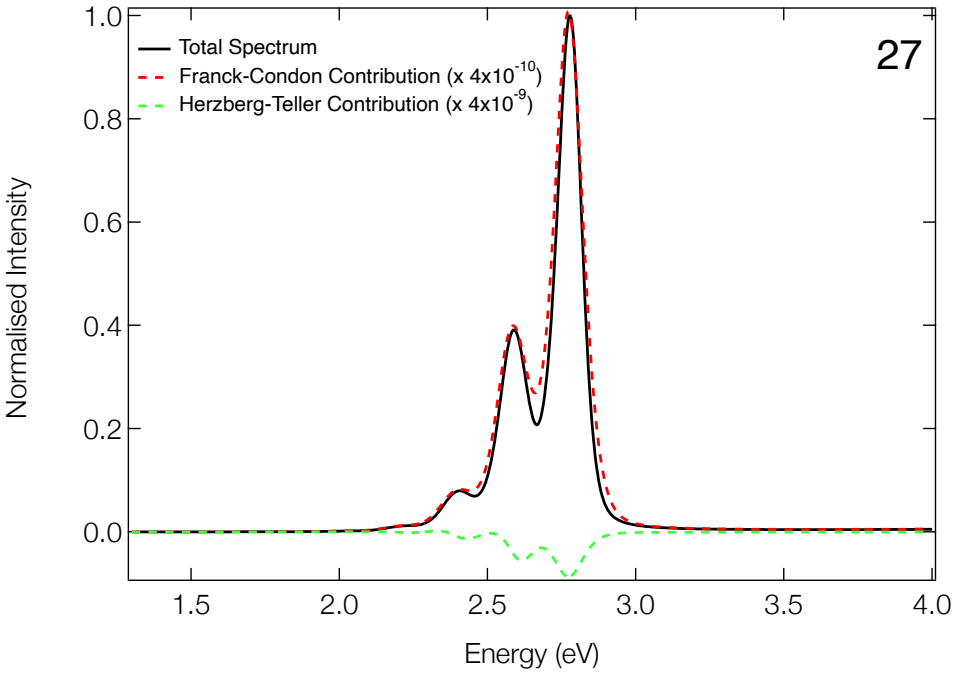

Figure S21: The computed emission spectrum of **27**.

S4 Supplementary Results: Density Differences

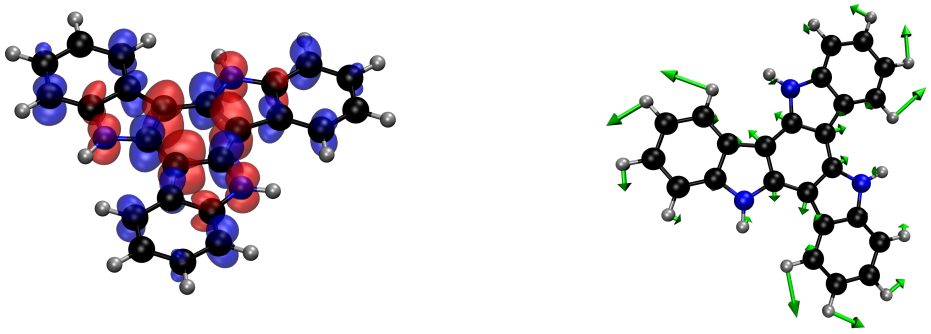

Figure S22: Left: The density difference of associated with the first singlet excited state of **1**. Right: Dominant normal mode responsible for the excited state structural change associated with **1**.

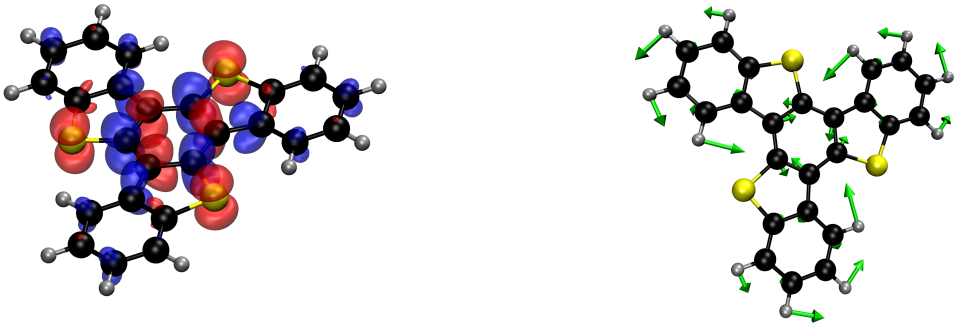

Figure S23: Left: The density difference of associated with the first singlet excited state of **2**. Right: Dominant normal mode responsible for the excited state structural change associated with **2**.

Figure S24: Left: The density difference of associated with the first singlet excited state of **3**. Right: Dominant normal mode responsible for the excited state structural change associated with **3**.

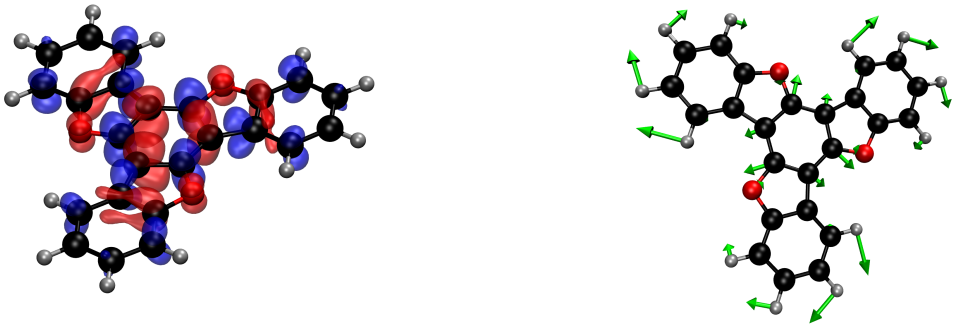

Figure S25: Left: The density difference of associated with the first singlet excited state of **4**. Right: Dominant normal mode responsible for the excited state structural change associated with **4**.

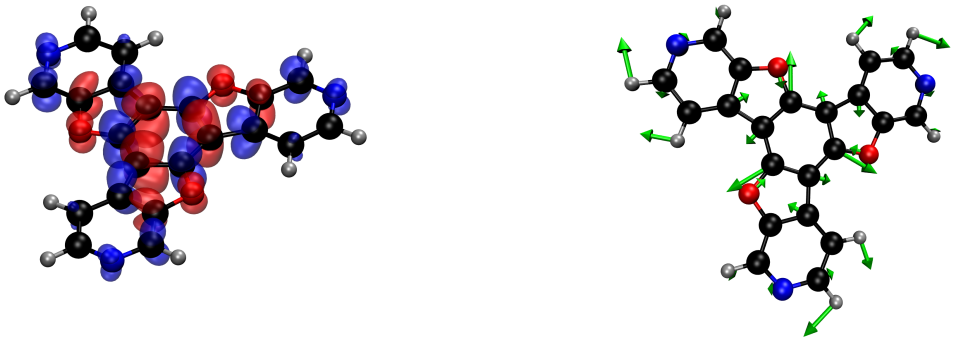

Figure S26: Left: The density difference of associated with the first singlet excited state of **5**. Right: Dominant normal mode responsible for the excited state structural change associated with **5**.

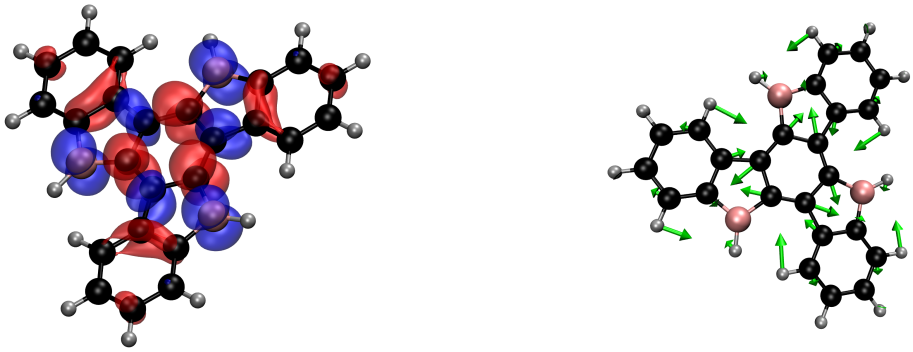

Figure S27: Left: The density difference of associated with the first singlet excited state of **6**. Right: Dominant normal mode responsible for the excited state structural change associated with **6**.

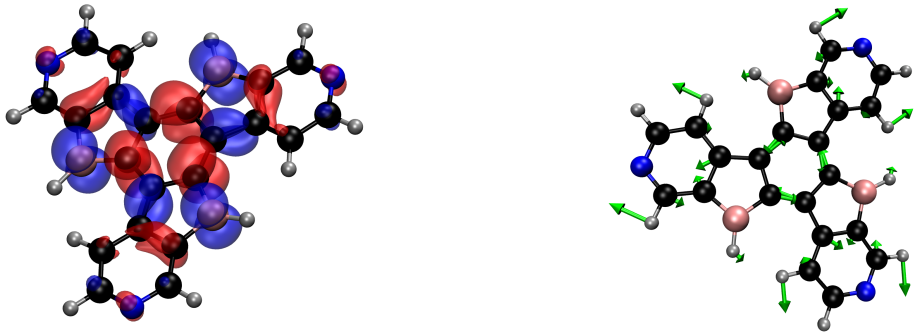

Figure S28: Left: The density difference of associated with the first singlet excited state of **7**. Right: Dominant normal mode responsible for the excited state structural change associated with **7**.

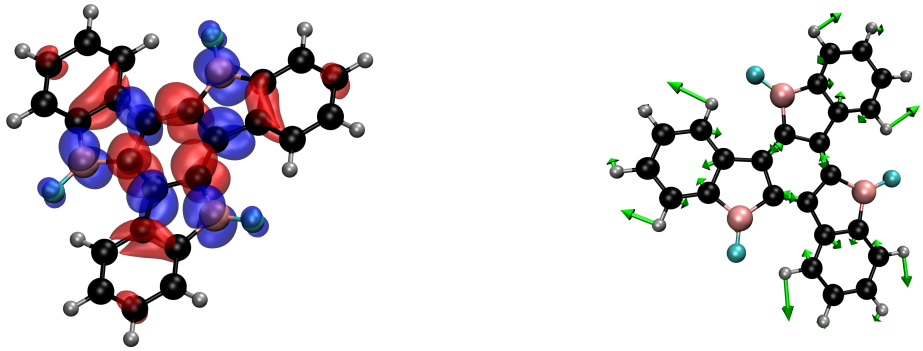

Figure S29: Left: The density difference of associated with the first singlet excited state of **8**. Right: Dominant normal mode responsible for the excited state structural change associated with **8**.

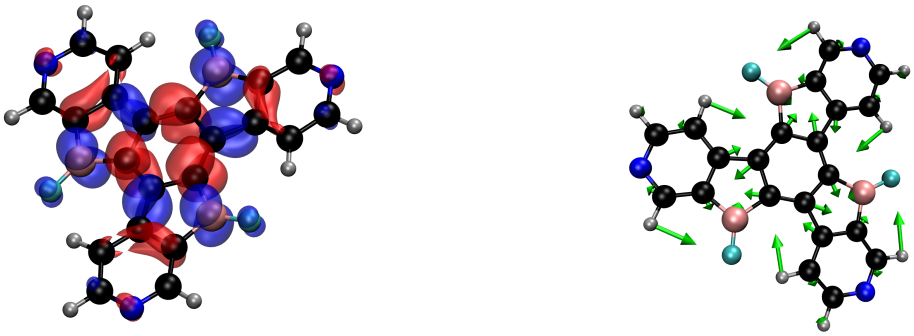

Figure S30: Left: The density difference of associated with the first singlet excited state of **9**. Right: Dominant normal mode responsible for the excited state structural change associated with **9**.

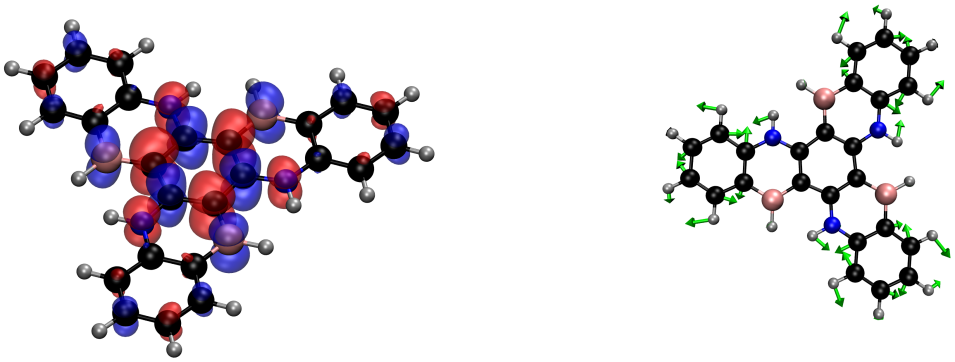

Figure S31: Left: The density difference of associated with the first singlet excited state of **10**. Right: Dominant normal mode responsible for the excited state structural change associated with **10**.

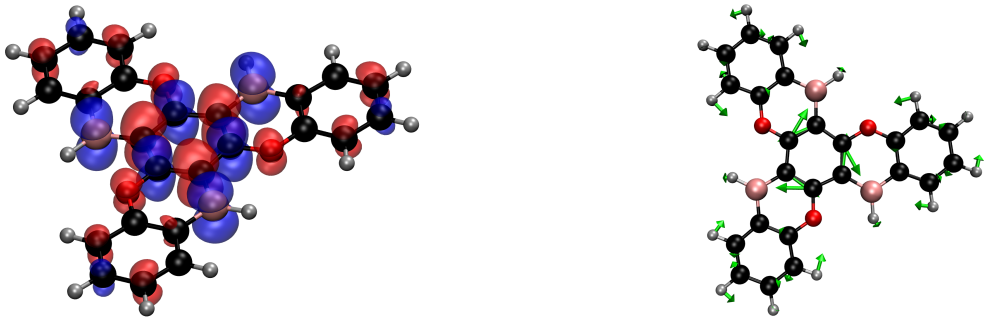

Figure S32: Left: The density difference of associated with the first singlet excited state of **11**. Right: Dominant normal mode responsible for the excited state structural change associated with **11**.

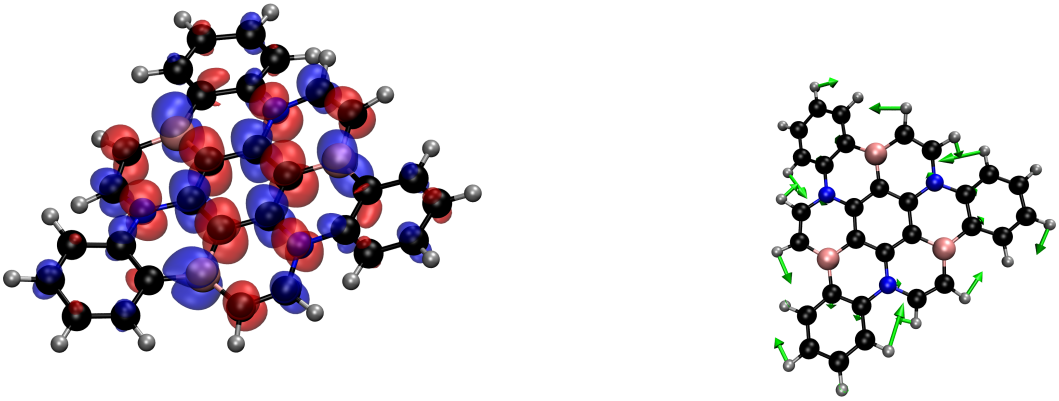

Figure S33: Left: The density difference of associated with the first singlet excited state of **12**. Right: Dominant normal mode responsible for the excited state structural change associated with **12**.

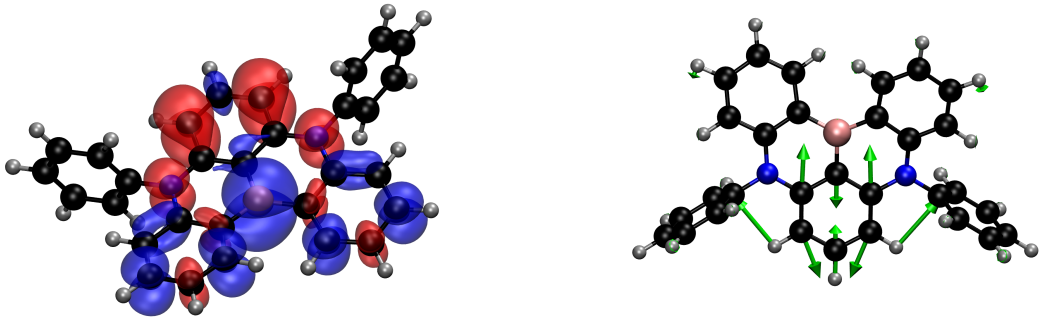

Figure S34: Left: The density difference of associated with the first singlet excited state of **13**. Right: Dominant normal mode responsible for the excited state structural change associated with **13**.

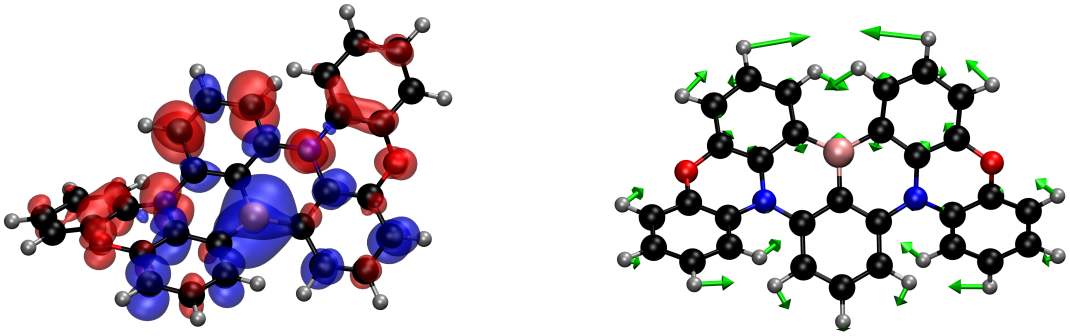

Figure S35: Left: The density difference of associated with the first singlet excited state of **14**. Right: Dominant normal mode responsible for the excited state structural change associated with **14**.

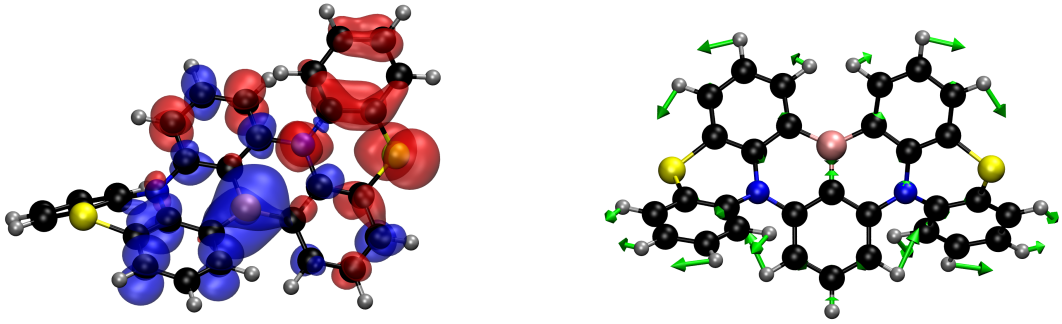

Figure S36: Left: The density difference of associated with the first singlet excited state of **15**. Right: Dominant normal mode responsible for the excited state structural change associated with **15**.

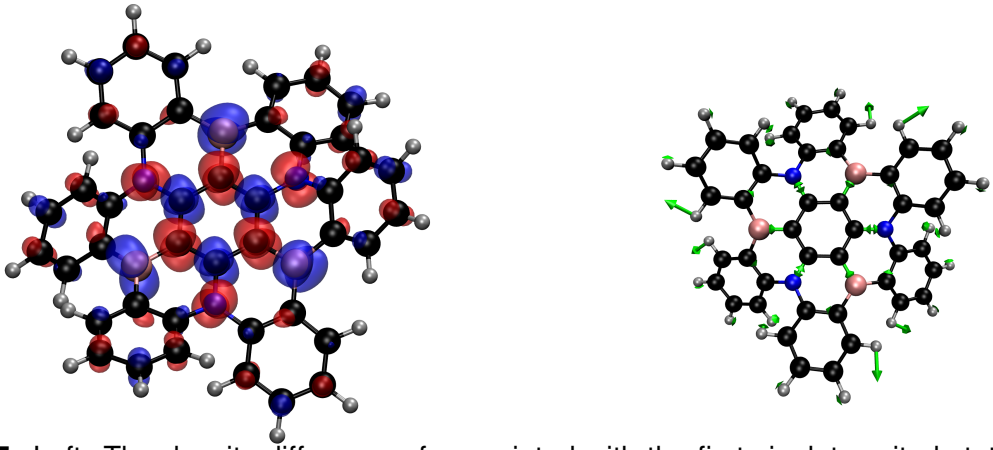

Figure S37: Left: The density difference of associated with the first singlet excited state of **16**. Right: Dominant normal mode responsible for the excited state structural change associated with **16**.

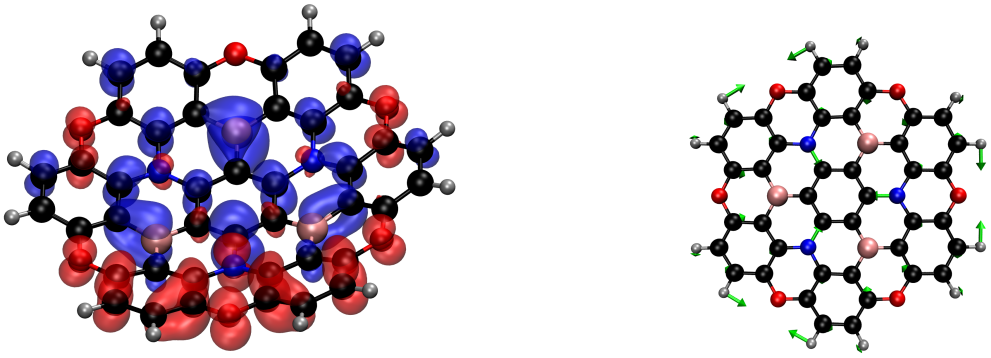

Figure S38: Left: The density difference of associated with the first singlet excited state of **17**. Right: Dominant normal mode responsible for the excited state structural change associated with **17**.

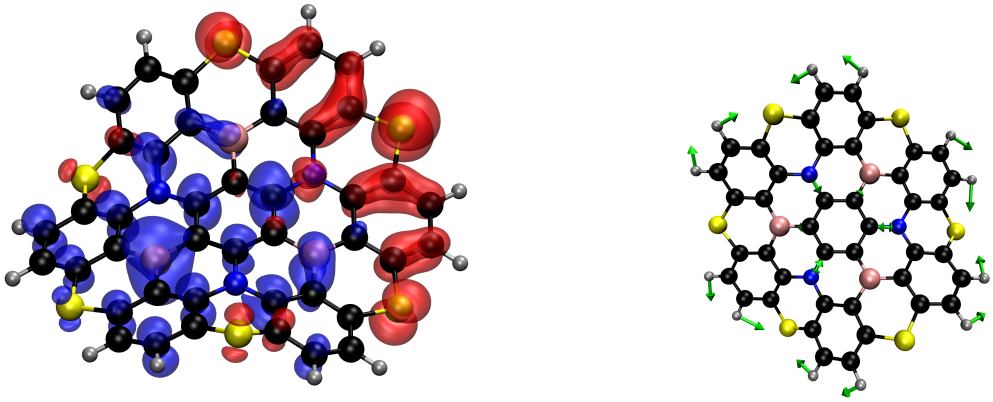

Figure S39: Left: The density difference of associated with the first singlet excited state of **18**. Right: Dominant normal mode responsible for the excited state structural change associated with **18**.

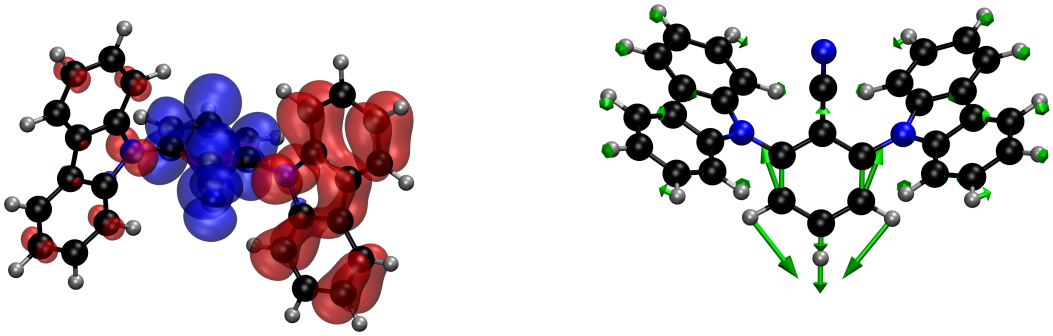

Figure S40: Left: The density difference of associated with the first singlet excited state of **19**. Right: Dominant normal mode responsible for the excited state structural change associated with **19**.

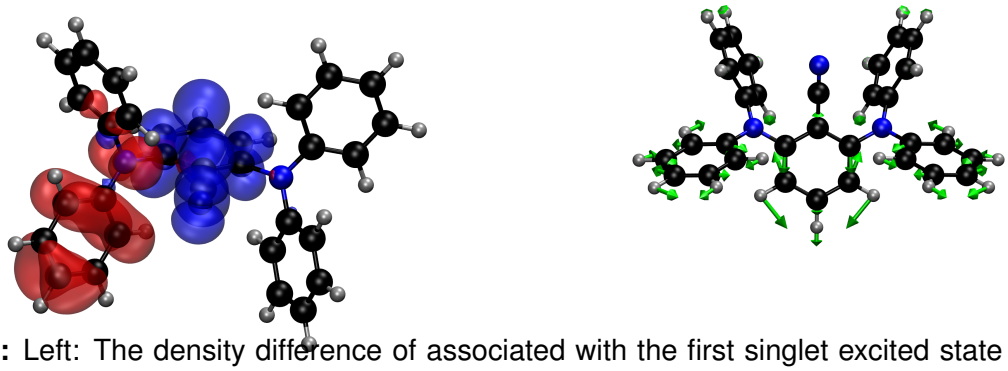

Figure S41: Left: The density difference of associated with the first singlet excited state of **20**. Right: Dominant normal mode responsible for the excited state structural change associated with **20**.

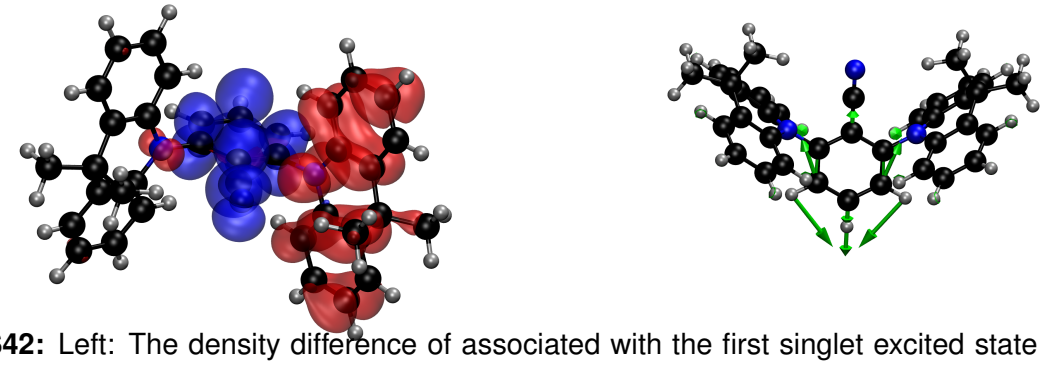

Figure S42: Left: The density difference of associated with the first singlet excited state of **21**. Right: Dominant normal mode responsible for the excited state structural change associated with **21**.

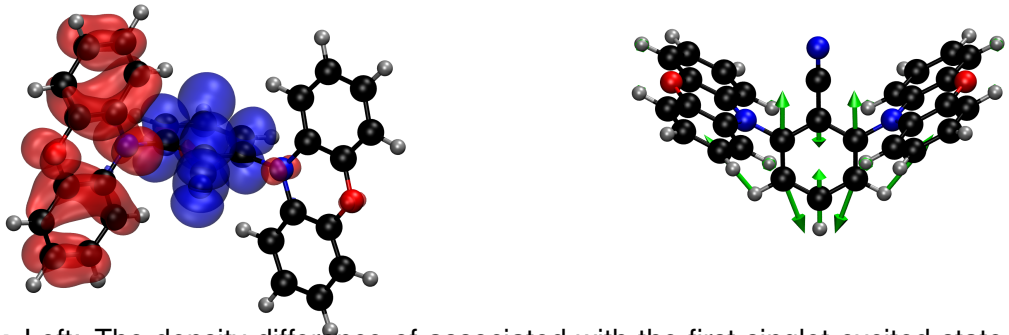

Figure S43: Left: The density difference of associated with the first singlet excited state of **22**. Right: Dominant normal mode responsible for the excited state structural change associated with **22**.

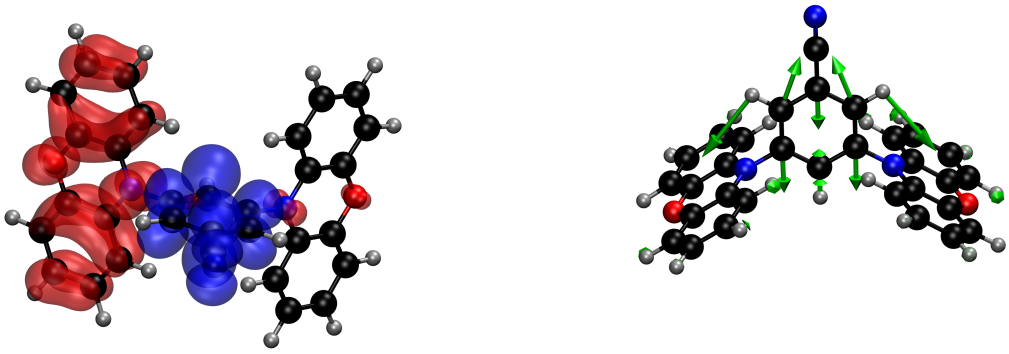

Figure S44: Left: The density difference of associated with the first singlet excited state of **23**. Right: Dominant normal mode responsible for the excited state structural change associated with **23**.

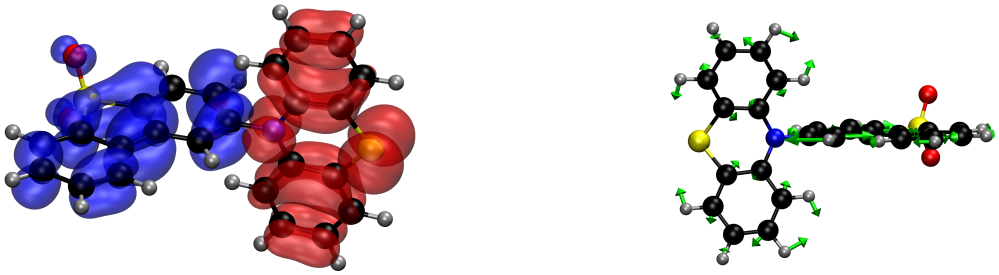

Figure S45: Left: The density difference of associated with the first singlet excited state of **24**. Right: Dominant normal mode responsible for the excited state structural change associated with **24**.

Figure S46: Left: The density difference of associated with the first singlet excited state of **25**. Right: Dominant normal mode responsible for the excited state structural change associated with **25**.

Figure S47: Left: The density difference of associated with the first singlet excited state of **26**. Right: Dominant normal mode responsible for the excited state structural change associated with **26**.

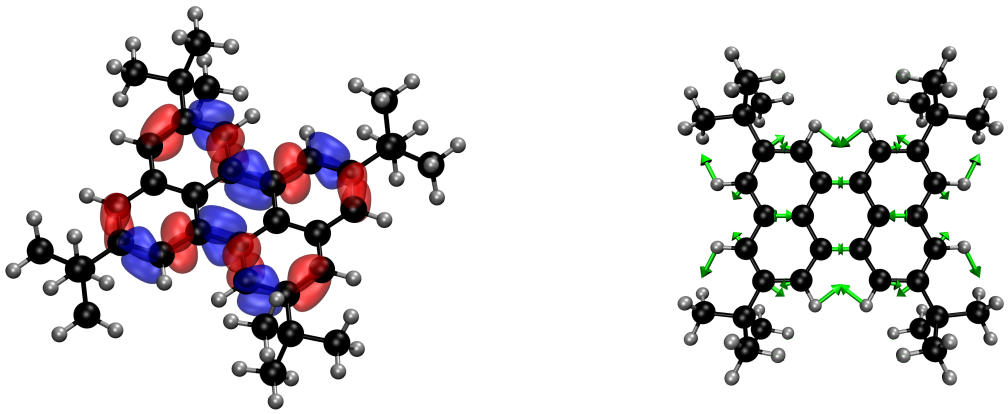

Figure S48: Left: The density difference of associated with the first singlet excited state of **27**. Right: Dominant normal mode responsible for the excited state structural change associated with **27**.

References

[1] Paloma L Dos Santos, Jonathan S Ward, Daniel G Congrave, Andrei S Batsanov, Julien Eng, Jessica E Stacey, Thomas J Penfold, Andrew P Monkman, and Martin R Bryce. Triazatruxene: A rigid central donor unit for a d–a3 thermally activated delayed fluorescence material exhibiting sub-microsecond reverse intersystem crossing and unity quantum yield via multiple singlet–triplet state pairs. *Advanced Science*, 5(6):1700989, 2018.

[2] Takuji Hatakeyama, Kazushi Shiren, Kiichi Nakajima, Shintaro Nomura, Soichiro Nakatsuka, Keisuke Kinoshita, Jingping Ni, Yohei Ono, and Toshiaki Ikuta. Ultrapure blue thermally activated delayed fluorescence molecules: efficient homo–lumo separation by the multiple resonance effect. *Advanced Materials*, 28(14):2777–2781, 2016.

[3] Tao Hua, Lisi Zhan, Nengquan Li, Zhongyan Huang, Xiaosong Cao, Zhengqi Xiao, Shaolong Gong, Changjiang Zhou, Cheng Zhong, and Chuluo Yang. Heavy-atom effect promotes multi-resonance thermally activated delayed fluorescence. 2021.

[4] Ramin Ansari, Wenhao Shao, Seong-Jun Yoon, Jinsang Kim, and John Kieffer. Charge transfer as the key parameter affecting the color purity of thermally activated delayed fluorescence emitters. *ACS Applied Materials & Interfaces*, 2021.

[5] Jonathan S Ward, Roberto S Nobuyasu, Andrei S Batsanov, Przemyslaw Data, Andrew P Monkman, Fernando B Dias, and Martin R Bryce. The interplay of thermally activated delayed fluorescence (tadf) and room temperature organic phosphorescence in sterically-constrained donor–acceptor charge-transfer molecules. *Chemical Communications*, 52(12):2612–2615, 2016.

[6] Tai-Sang Ahn, Astrid M Müller, Rabih O Al-Kaysi, Frank C Spano, Joseph E Norton, David Beljonne, Jean-Luc Brédas, and Christopher J Bardeen. Experimental and theoretical study of temperature dependent exciton delocalization and relaxation in anthracene thin films. *The Journal of chemical physics*, 128(5):054505, 2008.

[7] CA Parker and CG Hatchard. Delayed fluorescence of pyrene in ethanol. *Transactions of the Faraday Society*, 59:284–295, 1963.

[8] In HoáLee, Jun YeobáLee, et al. High efficiency blue fluorescent organic light-emitting diodes using a conventional blue fluorescent emitter. *Journal of Materials Chemistry C*, 3(34):8834–8838, 2015.